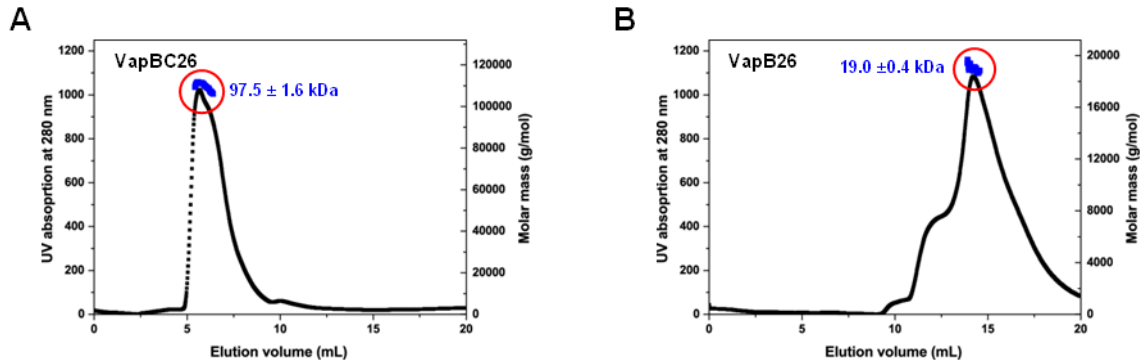

Supplementary Figure S1. Size-exclusion chromatography (SEC)-MALS chromatograms showing the oligomeric states of VapBC26 and VapB26 in solution. **(A)** VapBC26 was anticipated to form a hetero-octamer in solution, similar to its form in the asymmetric unit of the crystal structure. The UV absorption at 280 nm (left axis, black dotted line) and the calculated molecular weight (right axis, blue dotted line) are plotted as a function of the elution volume. The numbers next to the red circled peak indicate the average molecular weight obtained using MALS. **(B)** VapB26 was anticipated to exist as a dimer, similar to its oligomeric form in the VapBC26 complex.

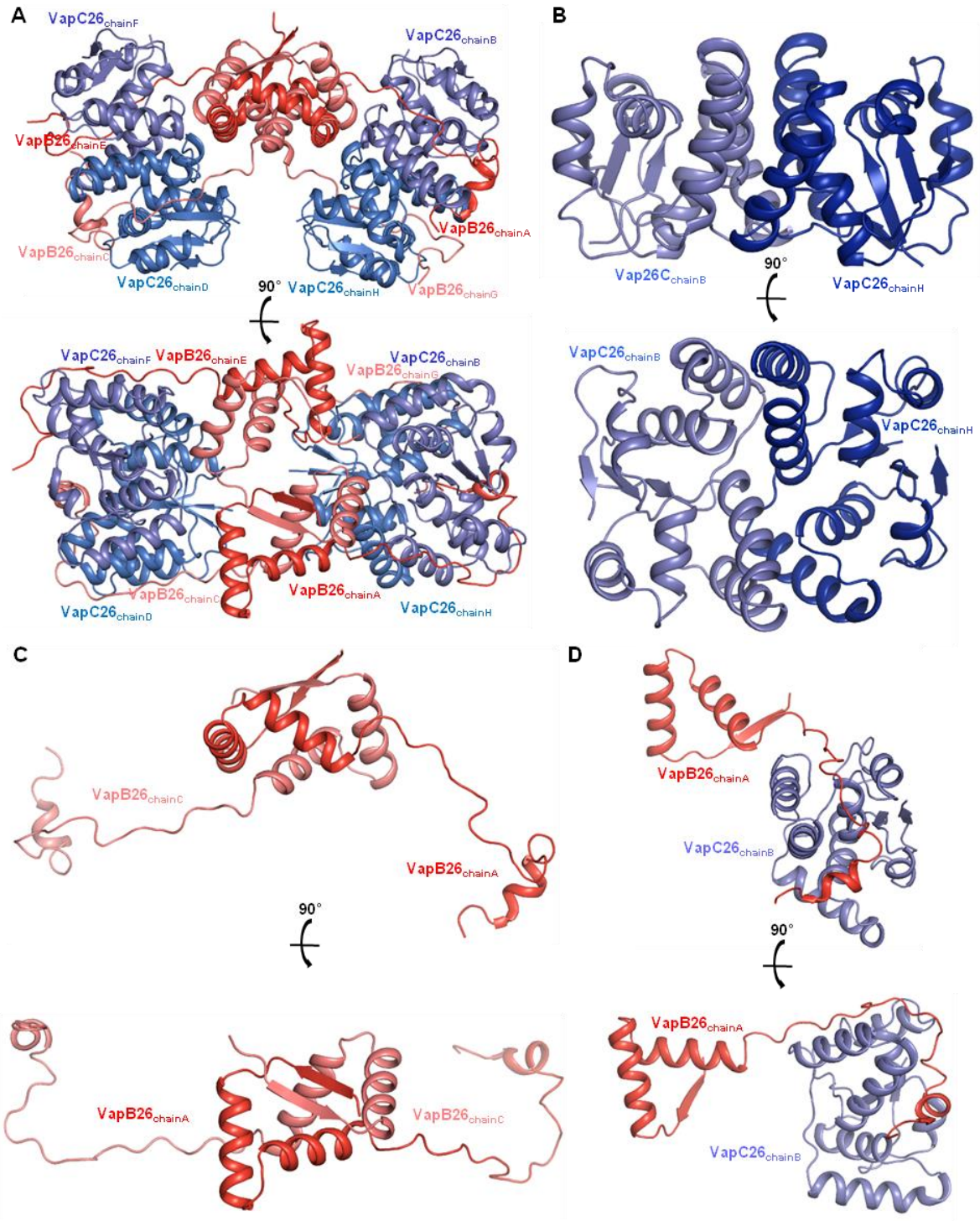

Supplementary Figure S2. Diverse point of view and 90° rotated diagrams of **(A)** VapBC26 hetero-octamer, **(B)** VapC26 dimer, **(C)** VapB26 dimer, and **(D)** VapBC26 heterodimer.

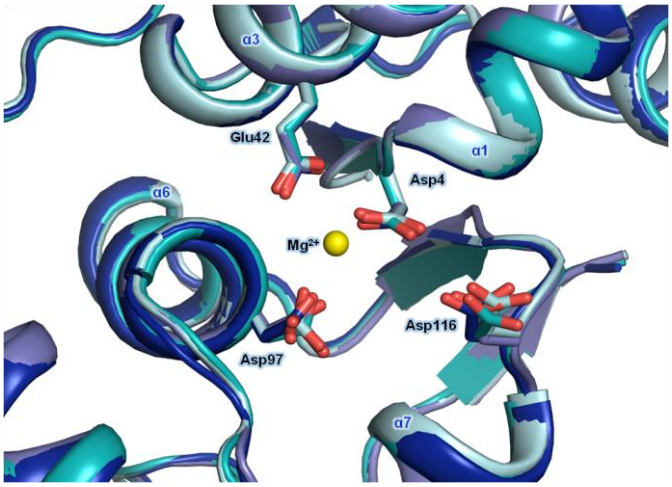

Supplementary Figure S3. Overlay of four toxin chains. The four active sites are composed of the same elements, but Mg^{2+} is observed only in chain H.

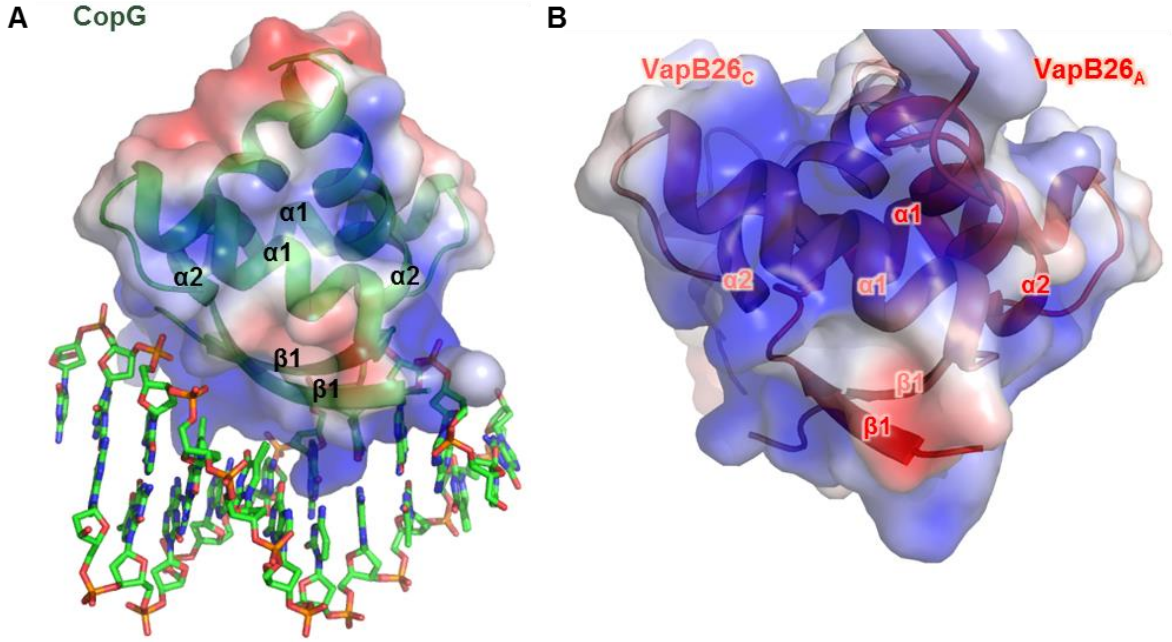

Supplementary Figure S4. Predicted conformation of VapB26-DNA interaction, showing the electrostatic potential surface. APBS method was used to calculate the electrostatic potential. **(A)** The structure of DNA bound CopG and its electrostatic potential surface. **(B)** The electrostatic potential of RHH domain of VapB26.

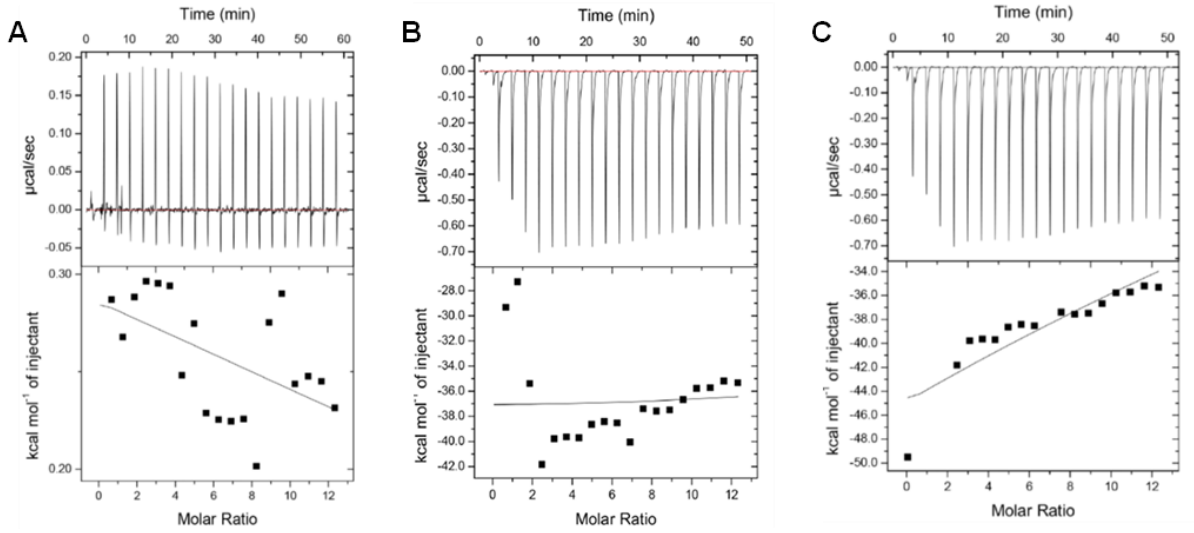

Supplementary Figure S5. ITC assay of VapB26 with control DNA and of VapBC26 with promoter DNA. The parameters could not be calculated. **(A)** ITC assay of VapB26 and control DNA, showing no interaction. **(B)** ITC assay of VapBC26 and promoter DNA in a buffer containing 500 mM NaCl and 250mM imidazole. **(C)** ITC assay of VapBC26 and promoter DNA in a buffer containing 400 mM NaCl.

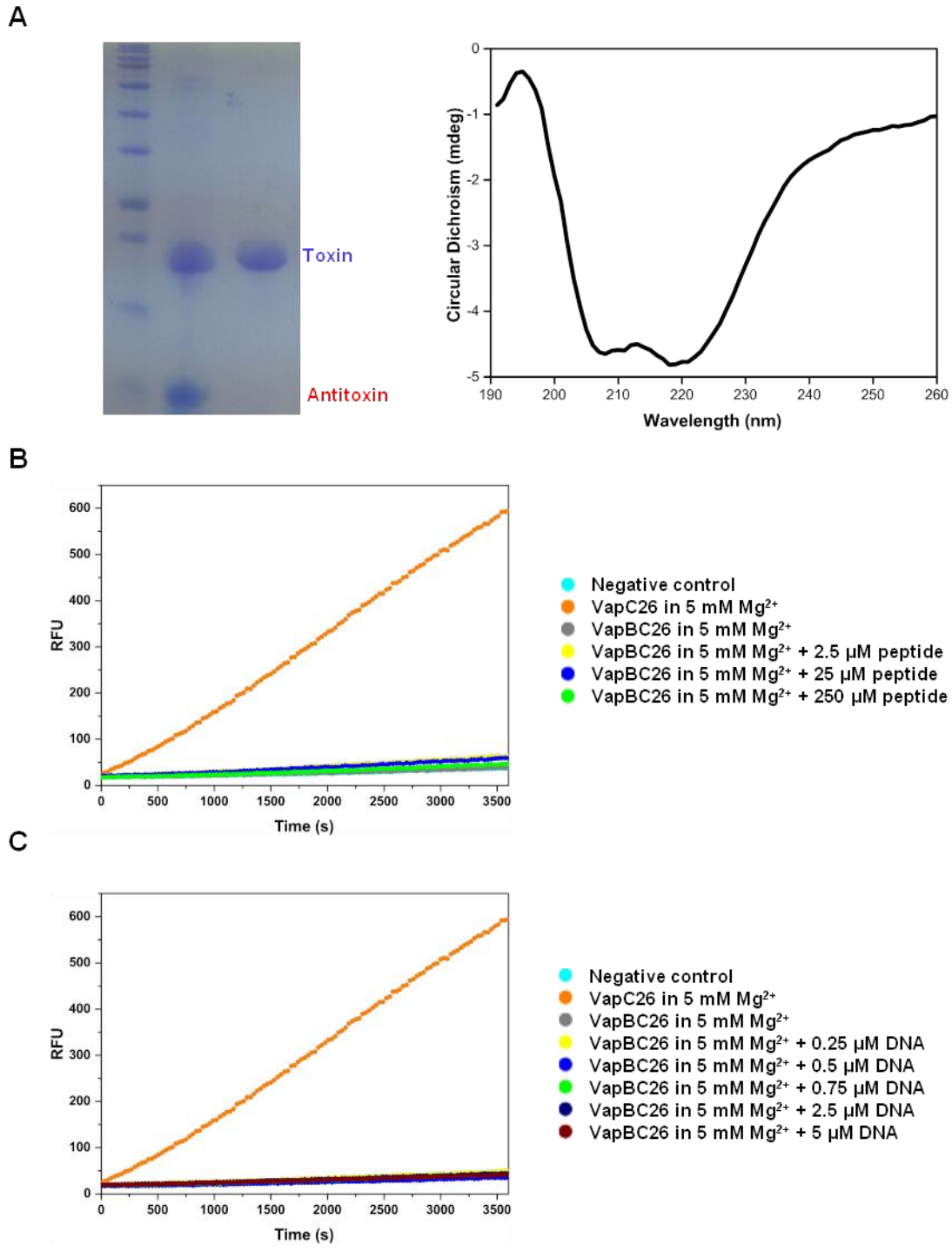

Supplementary Figure S6. Purity and structural integrity of VapC26 and ribonuclease activity of *M. tuberculosis* VapBC26. **(A)** Left: SDS-PAGE of the TA complex of VapBC26 (left) and purified VapC26 (right). Right : Circular dichroism (CD) data of VapC26, showing the maintenance of structural integrity. **(B), (C)** Ribonuclease activity of *M. tuberculosis* VapBC26 measured using the promoter DNA and the VapB26 mimic peptide 'PPPRGGLYAGSEPIA'. Fluorescence measurements, as a function of time, for VapBC26 in the presence of peptides and DNA. Forty units of RiboLock™ (Thermo Scientific) RNase inhibitor were used to prevent contamination. VapC26 was treated with EDTA prior to the

assay to remove metal ions. The negative control contained 50 mM Tris-HCl, pH 7.9, 500 mM NaCl, 250 mM imidazole, and 40 units of RiboLock™ (Thermo Scientific) RNase inhibitor. VapC26 in a solution containing 5 mM Mg^{2+} was used as a positive control. Each experiment was performed in triplicate. Neither peptides nor DNA contributed to increases in fluorescence. Other VapB26-mimicking peptides also did not have an impact on fluorescence.

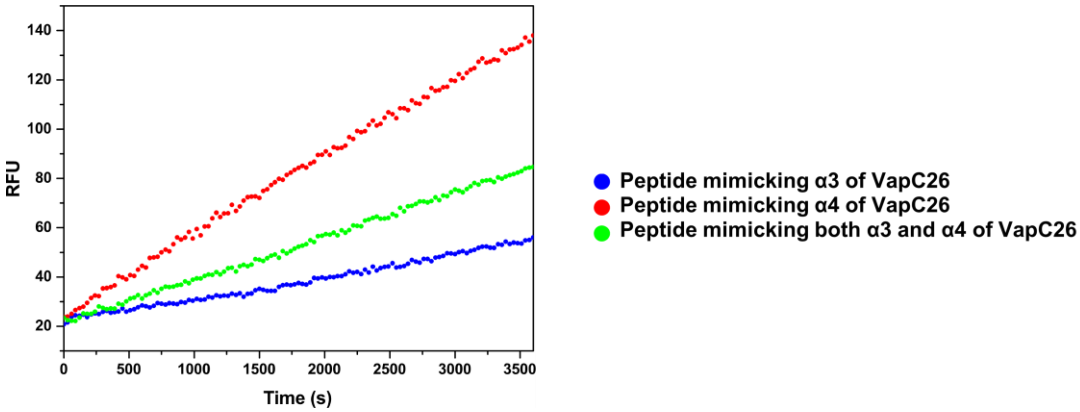

Supplementary Figure S7. Initial test of the RNase activity of *M. tuberculosis* VapBC26 in the presence of toxin-mimicking peptides (α3, α4 and both α3 and α4). When a synthetic RNA containing a fluorophore-quencher pair binds to VapC26, the RNA is digested and the quenching is removed. The released fluorophore generates fluorescence. The test was performed approximately 10 times on a smaller scale than in the standard experiments described in the main text to identify the most effective peptide. As shown in the diagram, the peptide that mimics the α4 helix has greater efficacy than the other two peptides.

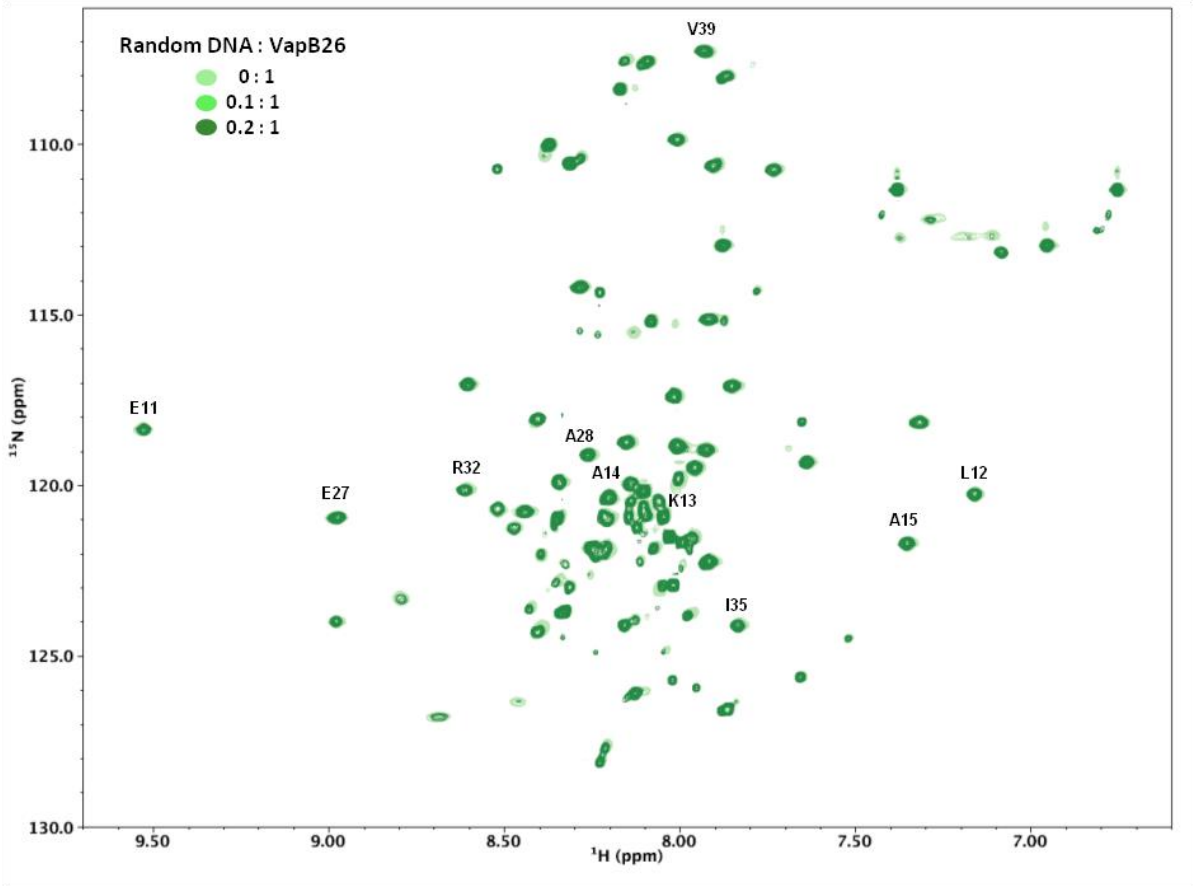

Supplementary Figure S8. NMR titration experiment of VapB26 and control DNA 'X'. Overlay of 2D ^{1}H-^{15}N HSQC spectra of 0.4 mM VapB26 with increasing ratios of added DNA 'X'. VapB26 with no DNA 'X' is shown in light green, VapB26 with 0.04 mM DNA 'X' is shown in medium green, and VapB26 with 0.08 mM DNA 'X' is shown in dark green. The peaks that displayed distinct changes during the interaction of VapB26 with promoter DNA are indicated. None of the indicated peaks show distinct changes in both the peak shifts and the intensity ratio in this spectrum.

Supplementary Table S1. Data-collection and refinement statistics for the SeMet and native structures.

(a) Data collection details. Values in parentheses are for the highest-resolution shell.

Data set	SeMet	Native
X-ray source	7A beamline of PLS, Korea	7A beamline of PLS, Korea
X-ray wavelength (Å)	0.9794	0.9795
Space group	$P4_1$	$P4_1$
Unit cell parameters		
a, b, c (Å)	64.22, 64.22, 216.13	64.35, 64.35, 216.96
α, β, γ (°)	90.0, 90.0, 90.0	90.0, 90.0, 90.0
Resolution range (Å)	30-2.65	50-2.55
Molecules per ASU	4 VapBC26 heterodimers	4 VapBC26 heterodimers
Observed reflections (>1σ)	619653	105433
Unique reflections	25229	27340
<I /σ(I)>	70.20 (10.87)[e]	34.98 (3.93)[e]
Completeness (%)	99.8 (100)[e]	94.9 (99.1)[e]
Multiplicity[a]	24.6 (25.4)[e]	3.9 (4.2)[e]
R_{merge} (%)[b]	11.3 (54.3)[e]	7.8 (67)[e]

(b) Refinement statistics

Data set	SeMet	Native
R_{work}[c] (%)	20.8	22.8
R_{free}[d] (%)	23.9	28.4
No. of atoms / average *B* factor (Å^2)		
Protein	6170 / 61.0	5978 / 79.8
Water oxygen	65 / 47.9	54 / 83.1
RMSD[f] from ideal geometry		
Bond distance (Å)	0.006	0.007
Bond angle (°)	1.25	1.27
Ramachandran statistics		
Most favoured regions (%)	96.2	95.5

Additional allowed regions (%)	3.7	4.4
Residues in disallowed regions (%)	0.1	0.1
MolProbity scrore	1.97 (98^{th} percentile)	1.82 (98^{th} percentile)
PDB accession code	5X3T	

[a] N_{obs}/N_{unique}

[b] $R_{merge} = \Sigma\ (I - \langle\ I\ \rangle)/\ \Sigma\ \langle\ I\ \rangle$

[c] $R_{work} = \Sigma_{hkl}\ ||F_{obs}| - k\ |F_{calc}||/\ \Sigma_{hkl}\ |F_{obs}|$

[d] R_{free} was calculated in the same manner as R_{work}, but with 5% of the reflections excluded from the refinement.

[e] The values in parentheses indicate the highest resolution shell.

[f] Root mean square deviation (RMSD) was calculated using REFMAC.

Supplementary Table S2. Primers used for mutation.

Primer	Sequence
P46A-F[a]	5’- GGCGGCGCCAAGCCGCCGGCGCGCGGGGGTCTATATGCG-3’
P46A-R[b]	5’- CGCATATAGACCCCCGCGCGCCGGCGGCTTGGCGCCGCC-3’
P46E-F[a]	5’- GGCGGCGCCAAGCCGCCGGAGCGCGGGGGTCTATATGCG-3’
P46E-R[b]	5’- CGCATATAGACCCCCGCGCTCCGGCGGCTTGGCGCCGCC-3’
Y51A-F[a]	5’- CCGCCGCGCGGGGGTCTAGCTGCGGGTTCGGAGCCCATC-3’
Y51A-R[b]	5’- GATGGGCTCCGAACCCGCAGCTAGACCCCCGCGCGGCGG-3’
Y51E-F[a]	5’- CCGCCGCGCGGGGGTCTAGAGGCGGGTTCGGAGCCCATC-3’
Y51E-R[b]	5’- GATGGGCTCCGAACCCGCCTCTAGACCCCCGCGCGGCGG-3’
L46A-F[a]	5’- GTAGCGGAACTCGACTATGCCGTCGCCACCCGGGTAGGT-3’
L46A-R[b]	5’- ACCTACCCGGGTGGCGACGGCATAGTCGAGTTCCGCTAC-3’
L46E-F[a]	5’- GTAGCGGAACTCGACTATGAGGTCGCCACCCGGGTAGGT-3’
L46E-R[b]	5’- ACCTACCCGGGTGGCGACCTCATAGTCGAGTTCCGCTAC-3’

[a,b] F and R indicate forward and reverse respectively. Enzyme sites are underlined above.

Supplementary Table S3. Structural comparisons with many parameters

S3A. Structural homologs of VapB26

Name	PDB code	r.m.s	Z-score	Sequence identity
VapB3 (*M. tuberculosis*)	3H87	5.4	4.1	16%
FitA (*N. gonorrhoeae*)	2BSQ	6.5	4.1	15%

S3B. Structural homologs of VapB26

Name	PDB code	r.m.s	Z-score	Sequence identity
VapC30 (*M. tuberculosis*)	4XGR	2.3	15.8	22%
VapC (*S. flexneri*)	3TND	2.4	14.2	16%
VapC15 (*M. tuberculosis*)	4CHG	2.4	13.7	24%
VapC (*R. felis*)	3ZVK	2.4	13.7	16%
VapC3 (*M. tuberculosis*)	3H87	2.5	12.1	18%
VapC5 (*M. tuberculosis*)	3DBO	2.7	11.3	23%

Supplementary Table S4. Residues used to create mimicking peptides

Residues (start - end)	Mimicked protein	Mimicked region
PPPRGGLYAGSEPIA (44-58)	VapB26	Coil between α2 and α3
VDELLAGF (61-68)	VapB26	α3
ALLAYFDAAEP (7-17)	VapC26	α1
PYVVAELDYLVATRVG (37-52)	VapC26	α3
DAELAVLRELAG (54-65)	VapC26	α4
YLVATRVGVDAELAV (45-59)	VapC26	Some moieties of α3 and α4
PYVVAELDYLVATRVGVDAELAVLRELAG (37-65)	VapC26	Whole α3 and α4

Supplementary Table S5. Predicted secondary structures with confidence scores offered by Talos based on the backbone-assigned amino acid sequence of VapB26

Sequence										M	D	K	T	T	V	Y	L	P	D
Predicted secondary structure										L	L	L	L	L	E	E	L	L	H
Confidence score										0	3	8	9	6	5	7	5	8	7
E	L	K	A	A	V	K	R	A	A	R	Q	R	G	V	S	E	A	Q	V
H	H	H	H	H	H	H	H	H	H	H	H	H	L	L	L	H	H	H	H
9	9	9	9	9	9	9	9	9	9	9	8	2	7	5	7	8	9	9	9
I	R	E	S	I	R	A	A	V	G	G	A	K	P	P	P	R	G	G	L
H	H	H	H	H	H	H	H	L	L	L	L	L	X	X	L	L	L	L	L
9	9	9	9	9	9	9	5	4	8	8	8	9	0	0	9	9	8	7	4
Y	A	G	S	E	P	I	A	R	R	V	D	E	L	L	A	G	F	G	E
L	L	L	L	L	L	L	L	L	L	L	L	L	L	L	L	L	L	L	L
8	8	9	0	0	9	9	8	7	4	5	8	9	9	9	8	7	7	7	8
R																			
L																			
0																			

H = helix, E = strand, L = coil, X = unassigned two prolines.

Confidence is scored from 0 (low) to 9 (high).